PAPER

Improving clogging predictions at managed aquifer recharge sites: a quantitative assessment on the vertical distribution of intrusive fines

Maria Chiara Lippera[1,3] · Ulrike Werban[3] · Thomas Vienken[2,3]

Abstract

Managed aquifer recharge (MAR) is an emerging approach to enhancing water storage capacity, improving water supply security and countering groundwater overexploitation. However, physical clogging, i.e. accumulation of suspended organic and inorganic solids within a sediment matrix, can lead to a significant reduction of infiltration rates and present difficulties in the functioning of MAR infrastructure. Clogging and subsequent reduction in infiltration capacity are often quantified based on monitoring data or field investigations, rather than on forecasts. Existing predictive models require specific parameterisation, making an application to heterogeneous sites, or under changing conditions, difficult. Hence, a generalised understanding of how intrusive fine particles distribute over depth during water recharge cycles for typical MAR infiltration basin sediments is needed to predict clogging susceptibility and clogging patterns already in the planning phase and before operation of MAR schemes. The study will contribute to operational reliability, deduce optimised management practices, and, ideally, reduce maintenance efforts. To achieve this goal, data from different soil-column clogging experiments are reviewed and complemented with experiments to establish a generally valid relationship for the vertical distribution of intrusive fines under consideration of the primary porous media's and intruding particles' characteristics. Obtained results allow for quantification of the amount of particles retained at the surface of the porous media, i.e. formation of a filter cake, a description of the distribution of fines over depth, and total clogging depth. Finally, the findings are applied to a real MAR case study site to showcase the quantification of clogging effects on recharge rates.

Keywords Managed aquifer recharge (MAR) · Clogging · Soil processes · Hydraulic properties

Introduction

Managed aquifer recharge (MAR) techniques are increasingly needed to enhance water storage capacity, improve water supply security and reduce impacts associated with fresh groundwater overexploitation (Dillon et al. 2018; Sprenger et al. 2017). The reduction in recharge rate due to clogging is one of the main concerns in the functioning of MAR systems (Bouwer 2002). Clogging originates from the accumulation of organic and inorganic suspended solids at the infiltration surface and in the migration of interstitial fines within the sediment matrix (Bennion et al. 1998; Goss et al. 1973; Wang et al. 2012). The particle size distribution of the infiltrating particles in relation to the pore bodies of the passed-through soil controls the shape of the clogging profile. Suspended particles with a larger particle size than the porous-media grain size accumulate on the surface of the granular material, forming the surface or external filter cake. Smaller suspended particles enter the interstitial space of the bed and deposit according to the mechanism of straining, leading to the occurrence of internal clogging. Straining is the blockage by fine particles at down-gradient pore constrictions that do not allow their passage (Bradford et al. 2003; Herzig et al. 1970). When fines intrude into the soil matrix, they increase the media surface area to volume ratio and reduce the media porosity (McDowell-Boyer et al. 1986). MAR sites can experience a decrease in infiltration

✉ Maria Chiara Lippera
  maria-chiara.lippera@tum.de

1 Technical University of Munich, TUM Campus Straubing
   for Biotechnology and Sustainability, Straubing, Germany

2 Weihenstephan-Triesdorf University of Applied
   Sciences, TUM Campus Straubing for Biotechnology
   and Sustainability, Straubing, Germany

3 UFZ - Helmholtz Centre for Environmental Research,
   Leipzig, Germany

capacity by orders of magnitude due to physical clogging (Racz et al. 2012). Often, sedimentation ponds reduce the concentration of suspended fines in the infiltration water; however, infiltration sites can accumulate fine particles transported from weathering reactions or from the rearrangement of deposits (Hutchison et al. 2013). The loss in performance can cause an increase in operation and maintenance costs (Dillon et al. 2016), the restoration of infiltration basins and boreholes (Martin 2013), and in extreme cases, the abandonment of the site (Hutchison et al. 2013). Ross and Hasnain (2018) report, for infiltration-basin recharged with untreated water, average MAR scheme costs of 0.77 USD capital cost per metre cubed recharged and a 0.13 USD operation and maintenance cost per metre cubed recharged. Despite these MAR schemes being relatively inexpensive to install, the costs for basin maintenance can be high, including the shut-down period for the cleaning and drying of passages (Ross and Hasnain 2018).

In the current state of the art of MAR clogging surveillance, instantaneous profile measurement systems of water content have been developed to accurately monitor reductions in infiltration capacity in the field (Barquero et al. 2019). Geophysical monitoring in MAR sites can track infiltration pathways by time-lapse electrical resistivity tomography (De Carlo et al. 2020; Nenna et al. 2014; Ulusoy et al. 2015). Thermal loggers and fiber-optic distributed temperature sensing assist in detecting spatial and temporal variations in infiltration rates (Becker et al. 2013; Mawer et al. 2016; Racz et al. 2012). Martin (2013) suggests observing the hydraulic responses in nearby observation wells during recharge to detect the presence of clogging (Pyne 1995). In MAR numerical simulations, the variation in hydraulic conductivity can be integrated through a time-variable scaling factor calibrated via an experimental setup (Glass et al. 2020). Although the up-to-date research improves basin management and clogging detection after development, there is still the necessity to design modelling tools to predict potential reductions in MAR infiltration capacity during the conceptual phase. So far, the basic water quality parameters used for MAR design have been total suspended solids (TSS), turbidity level for smaller particles (nephelometric turbidity units, NTU), and dissolved organic carbon (DOC) (Bouwer 2002; Dillon 2002; Okubo and Matsumoto 1983). However, the limit values of these parameters in reference to clogging can vary widely from site to site (Bouwer 2002).

Similarly, existing mathematical models for physical clogging and MAR design have been developed by fitting the breakthrough concentrations to the mass balance solution from a specific sand column setup (Torkzaban et al. 2015; Xie et al. 2020). The parametrisation derived from the column's breakthrough curves for a specific MAR site is not transferable to a different MAR context. The growing interest in MAR and its implementation worldwide requires further thorough studies into systematic clogging mechanisms and prevention (Zhang et al. 2020); hence, there exists a need to derive a general model for predicting physical clogging that can be adapted to multiple sites through site characterisation. Different factors determine the reductions in infiltration rates in the field—effluent water quality, basin soil texture, ponding depth, hydraulic loading rate and recharge cycles. However, the rate and degree of clogging are controlled mainly by the rate of suspended solids deposition, the size distribution of the fines and the size distribution of the receiving sediments (Hutchison et al. 2013).

One of the main obstacles in clogging research is predicting the characteristic depth of the particles' intrusion and deposition (Locke et al. 2001), thus the vertical distribution of fines within the porous media. Clogging profiles have already been expressed through an exponential decay function for sediment transport studies in hydraulically turbulent open channel flow (Cui et al. 2008; Huston and Fox 2015). Understanding how particles distribute along the porous media profile is essential in determining how fast and up to which depth the porous media will be severely clogged. The assessment of the site's susceptibility to clogging before construction prevents high unexpected costs and leads to evaluating the optimal design and operational options.

This study aims to improve physical clogging predictions by quantitatively assessing the distribution and volumes of deposited particles over soil depth during water recharge. The final scope is to determine the reduction in infiltration rates over the operational period of the infrastructure and the depth of the damage. To overcome the challenge of determining the characteristic depth of the particles' intrusion and deposition, the porous medium is hypothesised as a multilayer mesh in which a certain depth-varying percentage of particles are trapped, based on their diameter size, following an exponential decay. The novelty of this study is to propose an overall model to predict physical clogging, transferable to multiple MAR sites, while not relying on a specific set of parameters determined over a single-column experiment.

Therefore, results from existing column experiments in literature applicable to MAR conditions were reviewed and complemented with additional experiments to investigate whether a general relationship can be established between the vertical distribution of the fines and the porous-media and particle characteristics. The relevance of this work is highlighted by its application to the case study of a floodwater infiltration basin in Italy, assessing the risk of clogging and potential reductions in infiltration rates.

Methods

Literature review

To examine how intrusive fines distribute in porous media, available profiles of deposited fines were selected from

multiple-sand-column experiments. The experimental setup of these studies had to reflect MAR conditions, i.e., employing a porous media in the grain size range of coarse-medium sand (0.25–1 mm) and a low concentration of fine particles in suspension. In column experiments, constant head conditions best reflect the operating conditions for infiltration basins; however, in contrast, remobilisation of particles caused by the increase in injection pressure to overcome the resistance of the already declined hydraulic conductivity can be observed for column experiments under a constant flow rate. This behaviour is recognisable in the breakthrough curves from the increase of the relative concentrations of fines at the column effluent over time; hence, column experiments under a constant flow rate are less suitable for the analysis. In order to avoid high-water-pressure effects, the data derived from the sand column experiments under constant-head conditions described in Alem et al. (2014) were collected. The study under constant head conditions for 83 pore volumes (NVp) showed stable clay concentrations at the effluent; thus, the filtration action of the porous media did not change during the run of the column experiment. The experiments of Ahfir et al. (2017), for three sandy porous media in constant flow rate conditions, were also selected. Their study observed retention profiles for the duration of 3 NVp; thus, the clogged state of the porous media does not affect the vertical distribution of the fines yet, and the exerted water pressures are not further increased. Lastly, four-column experiments were run with artificial and natural material of defined grain-size ranges at the Helmholtz Centre for Environmental Research, Department of Monitoring and Exploration Technologies in Germany (Tippelt 2015). The experiments' scope was to observe the impact of fines input on the long-term infiltration capacity of a specific infiltration basin. In all three studies, the clay content was wet-sieved and weighed at the column sections, and the mass of fines deposited per unit of porous media mass was expressed as the retention profile.

In order to compare the datasets from the selected studies, the relative mass of deposited particles to the total mass of infiltrated particles was computed for each section. An averaged value over the section length was assumed at the central point to attribute the relative mass of deposited clay to a specific depth. Table 1 provides an overview of the setups of the column experiments from the selected studies. The number of datasets is limited by the availability of retention profiles in the literature. Filtration studies often lack this information since particle concentrations are conventionally automatically measured at the effluent. The lack of retention profile data in studies is indeed a limitation in understanding the straining and deposition processes occurring within the porous media. Retention profile data from experiments in gravel substrates were omitted, e.g. Gibson et al. (2009) and Tang et al. (2020). Due to the different experimental setups, the silt profiles in chromatography columns from Du et al. (2018) were also excluded. The latter case of silt particles depositing superficially in fine sand is indeed a case of interest for MAR site applications.

Experiments

Four experiments were additionally performed to increase the number of datasets and extend the analysis to the case of silt particles blocked at the porous media surface. A particle suspension was infiltrated in constant head conditions in sandy porous media in four grain-size ranges. The column of 4.8 cm in diameter and 50 cm in height had a constant head of 20 cm above the sand material for a total hydraulic gradient of 1.44 cm/cm. The experimental setup schematic is shown in Fig. 1a. The column was saturated from the bottom to avoid air trapping. After the outflow from the column reached stable conditions, the suspension was let to infiltrate at the concentration of 1 g/L. Differently from the other selected studies in Table 1, the experiments were performed with silt material, with a median diameter $d_{50} = 31.01$ (± 0.20) μm (Fig. 1b). The silt was previously obtained by dry-sieving a silty soil, and the particle size distribution was measured with laser diffraction (Cilas Particle Size 920). The suspension was allowed to infiltrate quartz sands in the grain-size ranges 0.5–1.0, 0.4–0.8, 0.2–0.7, and 0.1–0.4 mm (Euroquarz GmbH). An overview of the setup of the four experiments is reported in Table 1 under 'This study (2022)' followed by the experiment identifier number. The outflow of the column was measured with a precision balance scale (KERN PCB) and recorded via a USB to RS232 serial port. Turbidity values (NTU) for the column effluent were measured with a turbidimeter (HACH 2100P) to check the mass balance within the porous media. Previously a calibration was made between the known a priori suspended particles (SP) concentrations and the measured NTU values. At the end of the experiment, samples were taken at the column sections and at the porous media surface. The samples were dried and weighed, and the difference in weight was annotated after wet-sieving and drying.

Results

This section describes the analysis, modelling steps and results that contribute to assessing clogging profiles in porous media. The subsections are organized with the following contents:

Table 1 Experimental setups of the selected studies. The experiment identifier number distinguishes the single column experiments for the reference study. For each column experiment, the length and diameter of the column are indicated along with the number of sections in the column, the concentration of particles in the influent water, the num- ber of pore volumes infiltrated, the diameter size range of the sus- pended particles, the diameter size range of the porous media, median particles size of the suspension (d_{50}), and median diameter size of the porous media (D_{50})

Study reference and experiment ID	Column length (cm)	Column diameter (cm)	No. of sections	Concentra-tion (mg/L)	No. of pore volumes (NVp)	Size range (µm) and material -SP	Size range (µm) and material -PM	d50 (µm) -SP	D50 (µm) -PM
Ahfir et al. (2017) -1	62	4.4	15	500	3	2–30 kaolinite	315–630 sand	10	440
Ahfir et al. (2017) -2	62	4.4	15	500	3	2–30 kaolinite	315–800 sand	10	570
Ahfir et al. (2017) -3	62	4.4	15	500	3	2–30 kaolinite	630–800 sand	10	715
Alem et al. (2014)	40	4.5	9	250	83	1.7– 40 kao-linite	315–630 sand	15	410
Tippelt (2015) -1	50	30	5	102	30.78	0.36–103 bentonite	400–700 glass beads	7.68	530
Tippelt (2015) -2	50	30	5	102	30.78	0.36–103 bentonite	400–700 glass beads	7.68	530
Tippelt (2015) -3	50	30	5	102	30.31	0.36–103 bentonite	1,500 glass beads	7.68	1,500
Tippelt (2015) -4	50	30	5	102	23.44	0.36–103 bentonite	500–1,000 sand	7.68	710
This study (2022) -1	50	4.8	7	1,000	39.07	1–90 silt	500–1,000 sand	31	760
This study (2022) -2	50	4.8	7	1,000	40.43	1–90 silt	400–800 sand	31	590
This study (2022) -3	50	4.8	7	1,000	41.82	1–90 silt	200–700 sand	31	420
This study (2022) -4	50	4.8	7	1,000	32.51	1–90 silt	100–400 sand	31	230

Fig. 1 Information on the four performed experiments. **a** The column experimental setup, **b** particle size distribution (PSD) of the silt material used for the suspension
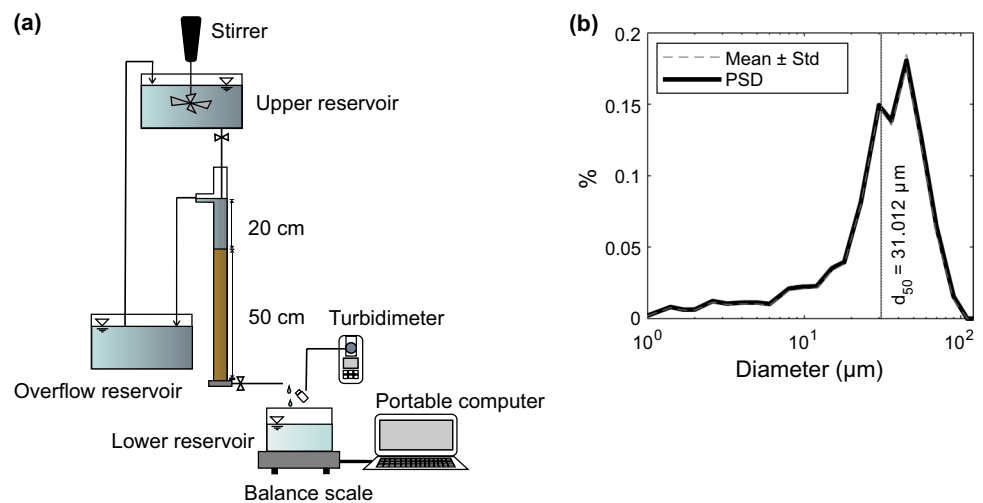
- Data analysis: retention profiles are expressed in relative masses of deposited fines over depth, and the vertical profiles are parametrized as exponential decay functions.

- A relationship is established between the relative mass of fines at the water–sediment interface and the geometric ratio d_{50}/D_{50} of the experimental setup.

- A mathematical solution defines the decay rate of fines deposition over depth. The expected depth of clogging and the clogging vertical profile are thus determined from the previously established relationship.
- For the experiments in superficial clogging conditions, the process leading to the external cake formation is formulated through a retention limit at the surface.
- The use of the Kozeny-Carman equation in computing reductions in soil permeability is tested for the observed outflow rates from the performed experiments.

An extensive discussion of the results is reported in section 'Discussion'.

Data analysis

From the literature review, three studies consisting of eight-column experiments reflecting MAR conditions were analysed, and four additional experiments were performed to extend the range of validity of the analysis. The profiles of deposited fines are expressed as the relative mass with respect to the total infiltrated mass of particles. The vertical distribution of the fines is outlined by an exponential decay function over the depth z (cm):

$$f(z) = f_{z=0} e^{-\alpha z} \tag{1}$$

with $f_{z=0}$ being the mass fraction of particles at the water–sediment interface and α being the decay rate, accounting for the reduction in the particles' retention per unit of depth:

$$\frac{df}{dz} = -\alpha f(z) \tag{2}$$

The fitting of the exponential decay curves to each clogging profile from the column experiments leads to the parameters describing the relative mass at the surface ($f_{z=0}$) and the decay rate of deposition (α). This formulation is valid for profiles not exceeding a saturation limit at the water–sediment interface, which corresponds to the maximum retention of fines. After this limit, the external cake starts forming. Therefore, only the experiments under internal clogging conditions are used to calibrate the parameters describing the clogging profiles. In Fig. 2, it can be observed that for greater deposition at the top of the column, a stronger fit to the exponential decay function is observed (Fig. 2a, e–g, i with respectively $R^2 = 0.97$, $R^2 = 0.93$ and $R^2 = 0.96$), in comparison to the other clogging profiles (Fig. 2b,c,h with $R^2 = 0.89$, $R^2 = 0.87$ and $R^2 = 0.70$). In contrast, the profile presenting the limit case for internal clogging, thus very

Fig. 2 Fitting of the exponential decay functions for the column experiment data from Tippelt (2015); **a–b** glass spheres 400–700 μm; **c** sand 500–1,000 μm, and **d** glass spheres 1,500 μm. Also, the condition used by Alem et al. (2014) and Ahfir et al. (2017); **e–f** sand 315–630 μm; **g** sand 315–800 μm, **h** sand 630–800 μm, and **i** This study (2022) sand 500–1,000 μm. The relative mass of fines $f(z)$ is the deposited mass (%) to the total mass of infiltrated particles per unit depth z. Above each graph are reported the values for $f_{z=0}$ (%) and α (%) from the exponential fit, and the coefficient of determination (R^2)
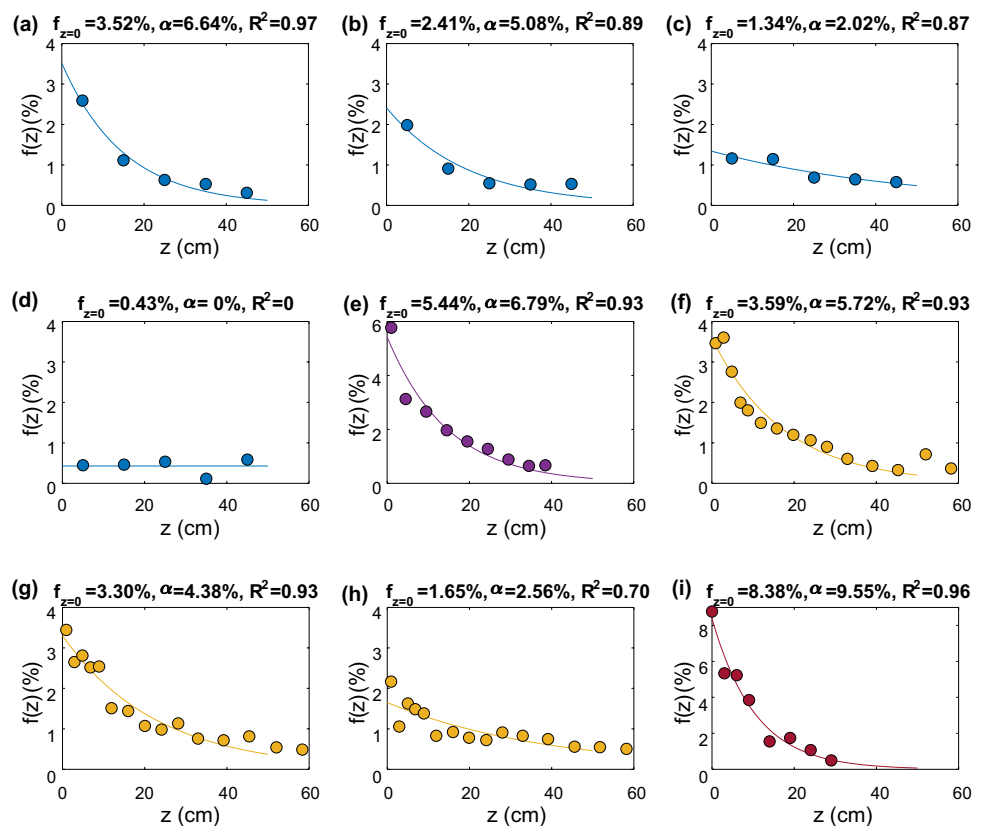
low deposition at the surface, does not show a variability around the mean value that can be explained by the exponential decay (Fig. 2d, $R^2 = 0$). The deposited fines are thus assumed to be distributed homogeneously through the soil with a decay rate α equal to zero. In the following sections, the exponential decay parameters are related to a geometric clogging predictor to explore the dependency of the clogging profile on the primary porous media and particle characteristics.

Clogging predictor

The parameters $f_{z=0}$ and α are related to the straining factors controlling the shaping of the retention profile; thus, predictors should summarise the primary porous-media and particle characteristics. Clogging predictors based on the system geometry account for the diameter of the suspended particles (d_p) relative to that of the porous media (d_g), i.e., d_p/d_g (see Gruesbeck and Collins 1982; Herzig et al. 1970; Khilar and Fogler 1998; Muecke 1979; Sakthivadivel 1969). In Bradford et al. (2003), the straining coefficient is a function of the ratio of the suspended solids' median particles size (d_{50}) to the porous media median grain size (D_{50}). Based on Bradford et al. (2003) the median diameter is assumed representative of the porous media and particles distribution. The median diameter is an immediate statistic to describe the particle size distribution, and it can be interpreted as a proxy for the average pore body size of the porous media (Mahmoodlu et al. 2016). The median diameters' values for the porous media grain distribution and suspended particles of each column experiment are reported in Table 1. For the retention profiles of the nine column experiments on internal clogging conditions, the relative mass of particles deposited at $z = 0$ cm is related to the geometric ratio d_{50}/D_{50}. The fraction of fines at the water–sediment interface follows a linear trend with increasing values of the geometric ratio d_{50}/D_{50} (Fig. 3).

The linear relationship verifies that fines retained superficially are close to zero for small median particle sizes to larger matrix grain diameters. The suspended particles with small size ranges intrude deeper into the soil formation, crossing a larger void space. Particles with larger median sizes instead lead to superficial clogging when intruding into a matrix with smaller grain diameters. Setting the boundary point at the origin ($f_{z=0} = 0$, $d_{50}/D_{50} = 0$), the following linear relationship for surface deposition at the water–porous media interface is established:

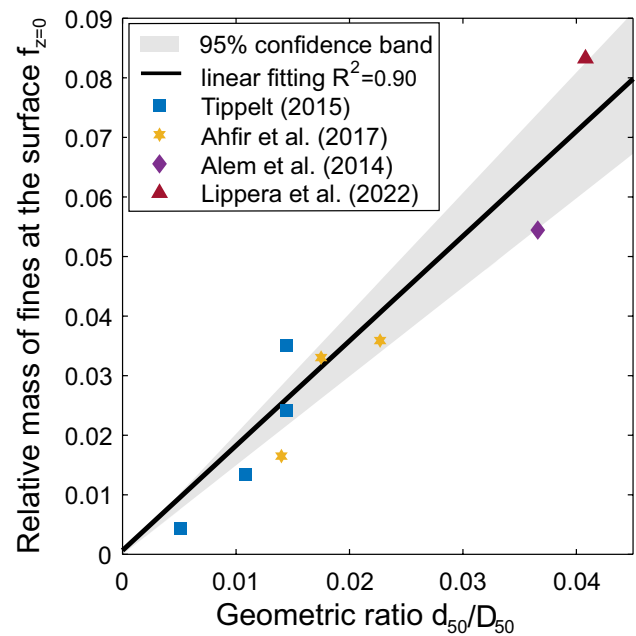$$f_{z=0} = 1.76 \frac{d_{50}}{D_{50}} \tag{3}$$

with $R^2 = 0.90$.

Fig. 3 Relationship between the relative mass of fines at the porous media's surface and the geometric ratio for the selected studies and one additional experiment under internal clogging conditions

The geometric ratio d_{50}/D_{50} provides systematic information on the relative mass of fines captured at the surface. The random error term is independent of the predictor d_{50}/D_{50} and has a mean value of zero, as proved by the one-sample t-test performed on the residuals ($p = 0.68$, H0: data are from a normal distribution with a mean equal to zero). Thus, the simple model with only the geometric ratio explains the variations in $f_{z=0}$. In order to assess whether Eq. (3) approximates the population regression line given the limited datasets, the model is tested with the leave-one-out cross-validation. Nine training data sets were generated, leaving out the data from one single-column experiment on which the model prediction is tested.

The unbiased estimates for the nine test errors in Table 2 provide an average MSE of 9.06e-05. The slope coefficients for the eight linear regressions fall within the 95% confidence interval of the full dataset relationship [1.49, 2.02]. Figure 3 reports the 95% confidence interval for the fitted linear regression with the full dataset.

Clogging depth and profile

In addition to the parameter $f_{z=0}$, the clogging profile is also defined by the decrease in relative mass over depth. The decay rate α expresses the exponential decay of captured particles over depth. Integrating from zero to infinite depth, for the function defining the fractions of retained fines up to the sum of 1, the following solution is obtained:

Table 2 Slope coefficients calibrated for the 9 datasets generated with the leave-one-out cross-validation method and mean square error (MSE) of the prediction on the excluded dataset

Parameter	Data set 1	Data set 2	Data set 3	Data set 4	Data set 5	Data set 6	Data set 7	Data set 8	Data set 9
Slope	1.78	1.75	1.78	1.73	1.76	1.76	1.77	1.87	1.59
MSE	2.06E-05	5.83E-06	7.20E-05	1.03 E-04	2.04E-06	2.24E-05	3.29E-05	1.97E-04	3.60E-04

$$\int_{0}^{\infty} f_{z=0} e^{-\alpha z} dz = 1 \tag{4}$$

$$\left[\frac{f_{z=0} e^{-\alpha z}}{-\alpha} \right]_{0}^{\infty} = 1 \tag{5}$$

$$\alpha = f_{z=0} \tag{6}$$

Equation (6) shows that the reduction factor per unit of depth α is directly correlated to the fraction of retained fines at the surface $f_{z=0}$, and the data from the eight retention profiles in Fig. 2 confirm this relationship with an $R^2 = 0.59$ and RMSE = 0.0169. Part of the error might be attributed to the fact that the entire mass of intrusive fines is not recovered in all the experiments. It is preferable to adopt the mathematical solution for the calibration of α, to guarantee that the defined fractions of fines amount to one over the total porous media depth. Equation (6) verifies that for an extreme condition in *surface* clogging, the retention decreases steeply with depth ($\alpha = f_{z=0} \approx 1$), and the soil exhibits a short clogging profile. By contrast, the soil exhibits a deep clogging profile for an extreme condition in *internal* clogging ($f_{z=0} = \alpha \approx 0$), and a constant fraction of suspended particles is retained with depth. The clogging depth can also be assessed for intermediate conditions of the clogging profile. Assuming 0.5% retained fines as an arbitrary threshold for ending the clogging profile, the depth of clogging z_{clog} (cm) is:

$$z_{\text{clog}} = -\ln \left(\frac{0.005}{f_{z=0}} \right) \frac{1}{\alpha} \tag{7}$$

with $f(z_{\text{clog}}) = 0.005$ being the relative mass at the bottom of the clogging profile.

Thus, the fines-fraction profile through the sediment matrix can be estimated only from the ratio of the median particle diameter size to the median grain diameter size. Substituting in Eq. (1) the parameters $f_{z=0}$ and α from the linear regressions reported in Eqs. (3) and (6), the final equation describing the clogging profile is:

$$f(z) = \left(1.76 \frac{d_{50}}{D_{50}} \right) \exp \left(-1.76 \frac{d_{50}}{D_{50}} z \right) \tag{8}$$

This formulation expresses the fractions of particles captured along the porous media's depth, as long as the

saturation limit at the water–sediment interface is not reached and particles intrude internally.

External cake formation

The relationship for the clogging profile (Eq. 8) can be adopted for internal clogging only since it does not account for the formation of the external cake. In surface clogging conditions, after exceeding a saturation limit for the fines' retention at the surface, the porous media would start accumulating the fines at the top. The overall amount of fines depositing externally of the porous media would diverge from the retention profiles expressed in relative mass. The fines in excess at $z = 0$ are dependent on the total amount of infiltration fines after the retention limit at the water–sediment interface has been reached. In this regard, the three performed experiments in surface clogging conditions are used for validation. It is assumed that the particles would start distributing internally during infiltration, according to Eq. (8), up to a total mass of infiltrated particles, after which the formation of the external cake begins. The mass retained at the porous media surface, after which particles stop intruding internally, can be defined as $M_{z=0,\text{limit}}$:

$$M_{z=0,\text{limit}} = f_{z=0} M_{\text{tot,limit}} \tag{9}$$

with $M_{\text{tot,limit}}$ (g) the total mass of infiltrated particles up to the limit of the external cake formation. The retention limit at the porous media surface can be approximated by the volume of voids V_{v} (cm). This volume at the water–sediment interface, is defined for the infiltration area A (cm) with the radius of the median grain (cm):

$$V_{\text{v}} = An \frac{D_{50}}{2} \tag{10}$$

with the porosity n of the porous media. The void space is filled with particles having bulk density ρ_{s} (g/cm^3); thus, the maximum retained mass at the water–sediment interface is:

$$M_{z=0,\text{limit}} = V_{\text{v}} \rho_{\text{s}} \frac{d_0}{d_{50}} \tag{11}$$

the parameters D_{50} (cm) and d_{50} (cm) account for the straining effect given by the proportion of the median particle diameters to the average pore diameter $d_0 = 0.235 \, D_{50}$ (Mahmoodlu et al. 2016). Combining Eqs. (9) and (11), the

input of fines after which the external cake would start forming is the following:

$$M_{\text{tot,limit}} = \frac{An\rho_s 0.117D_{50}{}^2}{d_{50}f_{z=0}} \tag{12}$$

with $f_{z=0}$ from Eq. (3).

The particles' profile in superficial clogging conditions is thus corrected to account for the formation of the external cake:

$$f(z) = \left(1.76\frac{d_{50}}{D_{50}}\right) \exp\left(-1.76\frac{d_{50}}{D_{50}}z\right)\frac{M_{\text{tot,limit}}}{M_{\text{tot}}} + \frac{M_{\text{tot}} - M_{\text{tot,limit}}}{M_{\text{tot}}}(z=0) \tag{13}$$

with M_{tot} (g) the total infiltrating mass of particles. The equation is applied to the observed clogging profiles from the three experiments exhibiting superficial clogging, as shown in Fig. 4. The model predicts the observed relative masses of fines at the column sections with RMSE values of 0.0119, 0.0152 and 0.00902. This formulation closes the gap in predicting soil permeability reductions at discrete depths and the overall decrease in infiltration capacity.

Permeability reductions

The previous section described the formulation for the quantitative assessment of the vertical distribution of fines. Estimating the volume of intruded and deposited particles at discrete depths improves models that predict the evolution of soil infiltration capacity. When particles intrude into the soil matrix, the media surface area to volume ratio is increased, and the soil porosity is reduced, leading to a decrease in soil permeability. Most clogging studies conducted for engineering purposes (Alem et al. 2013; Blazejewski and Murat-Blazejewska 1997; Federico 2017; Herzig et al. 1970; Locke et al. 2001; Reddi et al. 2000) rely on the Kozeny-Carman equation (Carman 1937; Kozeny 1927) to compute the reduction in soil permeability. The model that provided a greater fit to the flow decrease observed from the column experiments is the one proposed by Alem et al. (2013):

$$\frac{k(z,t)}{k_0} = \frac{n(z,t)^3}{n_0^3}\frac{(1+n_0)^2}{(1+n(z,t))^2}\frac{S_0^2}{S(z,t)^2}\left(\frac{T_0}{T(z,t)}\right)^2 \tag{14}$$

with n the porosity, S the specific surface area per unit volume of particles (1/cm) and T the tortuosity (cm/cm). For more details on Eq. 14, please refer to Alem et al. (2013).

The physical characteristics of the porous media evolve along with the volume of particles intruded, expressed per unit of porous media volume, as:

$$\sigma(z,t) = \frac{M_{\text{tot}}(t)}{Al\rho_s}f(z) \tag{15}$$

with $M_{\text{tot}}(t)$ the total infiltrated particles up to time t, $f(z)$ from Eqs. (8) and (13), ρ_s the particles' specific density (g/cm^3), A the infiltrating area (cm) and l the unit depth (cm). The decrease in porosity of the porous media follows the formulation from Herzig et al. (1970):

$$\frac{n(z,t)}{n_0} = 1 - \frac{\beta\sigma(z,t)}{n_0} \tag{16}$$

with β the inverse of the compaction factor of retained particles $\beta = 1/(1-n_d)$. The porosity of the retained fines n_d is derived from the average densities of deposited particles (Alem et al. 2013; Boller and Kavanaugh 1995).

For the total infiltrated suspension with a concentration of 1 g/L of suspended particles, the recorded outflow rates at the column were converted into total permeability reduction given the constant gradient. The decrease in soil permeability modelled according to the Kozeny-Carman equation (Eq. 14) explains the observed total variation in permeability at the column, as shown in Fig. 5.

The decrease in soil permeability shown in Fig. 5 has been modelled from the estimated vertical distribution of fines based on the geometric ratios d_{50}/D_{50} (Eqs. 8 and 13). The limit at which particles start accumulating superficially, forming the external cake, is computed from Eq. (12). For the reduction in permeability at discrete depths (Eq. 14), the total reduction in permeability in the internal clogging conditions (Fig. 5a) is:

Fig. 4 The clogging profiles from Eq. (13) under superficial clogging conditions are tested for the observed relative mass of fines (%) deposited over depth for the experiments of This study (2022) **a** sand 0.4-0.8 mm, **b** sand 0.2-0.7 mm and **c** sand 0.1-0.4 mm
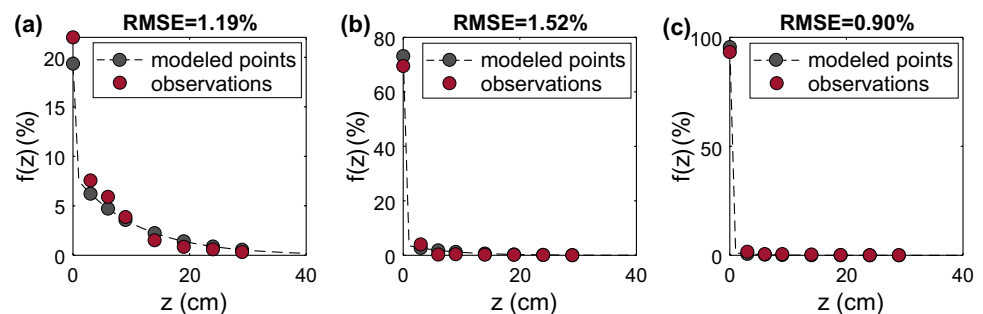
Fig. 5 The model prediction from the Kozeny-Carman equation for permeability decrease k/k_0 compared with the observed reduction in permeability from the column outflow during the experiments of This study (2022): **a** sand 0.5–1 mm, **b** sand 0.4–0.8 mm and **c** sand 0.2–0.7 mm, **d** sand 0.1–0.4 mm. The red vertical line indicates the retention limit at which the external cake starts forming
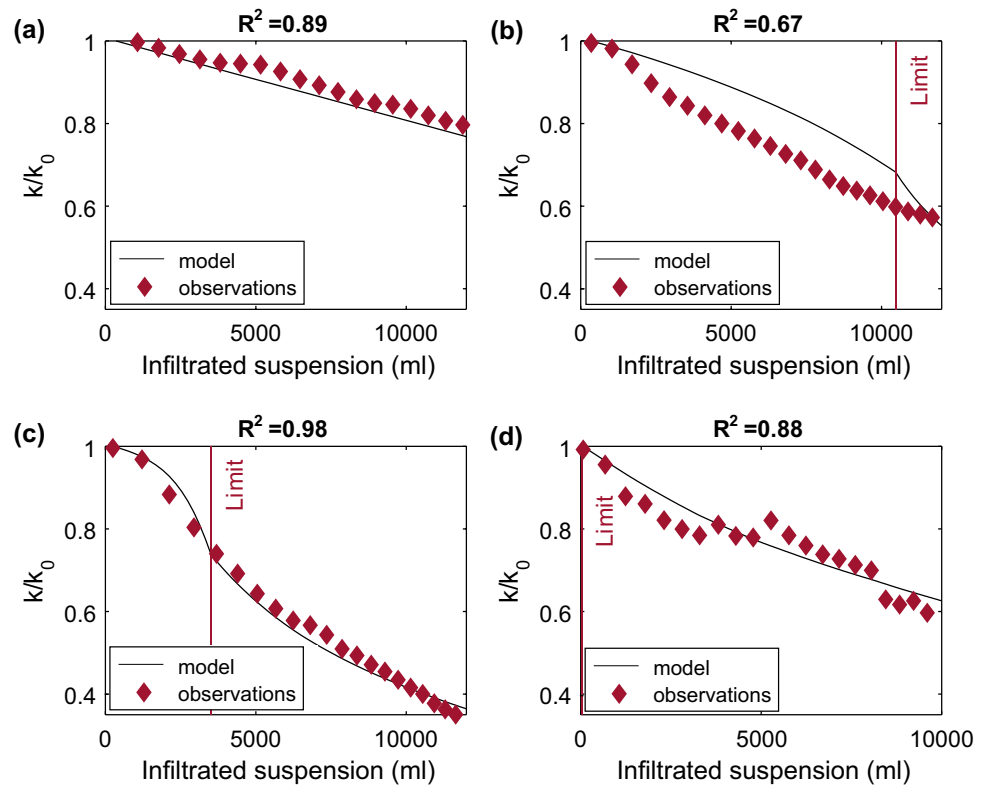
$$\frac{k_{\text{tot}}(t)}{k_0} = \frac{L}{\sum_{z=0}^{L} \frac{l}{\frac{k(z,t)}{k_0}}} \tag{17}$$

with L the total length of the porous media and $k(z,t)/k_0$ the permeability's reduction per unit depth l.

In superficial clogging conditions (Fig. 5b,c,d), the total decrease in permeability is computed by accounting for external cake layering:

$$\frac{k_{\text{tot}}(t)}{k_0} = \frac{L + L_{\text{cake}}(t)}{\sum_{z=0}^{L} \frac{l}{\frac{k(z,t)}{k_0}} + \frac{L_{\text{cake}}(t)}{\frac{k_{\text{cake}}}{k_{z=0,\text{limit}}}}} \tag{18}$$

with $L_{\text{cake}}(t)$ being the thickness of the external cake, $k_{z=0,\text{limit}}$ the permeability of the porous media at the surface when $M_{z=0,\text{limit}}$ is met, and k_{cake} a calibrated parameter associated with the permeability of the fines depositing superficially. For all three experiments under surface clogging conditions (Fig. 5b,c,d) one unique calibrated value was set: $k_{\text{cake}} = 0.0003$ (cm/s).

The previously shown equations can be implemented to develop a model for physical clogging at MAR sites. The profile of the damage and the time for the facility to be clogged can be estimated from parameters collected in the field. The application of these findings is illustrated in the next section, in order to estimate the evolution in infiltration rates due to the input of fines at a MAR field site.

MAR application

This section showcases how MAR operators can implement the findings in section 'Results' in order to assess the site's vulnerability to clogging. The clogging depth and the evolution over time in infiltration rates can be deduced from the hydraulic loading of several flooding events. In this scenario analysis, no maintenance is performed at the MAR site. The Loria infiltration test site is presented with the sole intention of highlighting the applicability of the results. The site is situated approximately 15 km north of Cittadella in the Province of Padua, Italy, within the catchment area of the river Brenta, and the source for infiltration is flood water of the Lugana stream. The long-term infiltration capacity of the site is susceptible to physical clogging due to eroded clays reaching the pond during flood events. This MAR scheme does not comprise a sedimentation pond; thus, the transported clay is deposited as a soil overlay. For further information on the site, see P.A.T.I. (2013), Fontana et al. (2014) and Tippelt (2015). For the Tippelt (2015) study, four representative soil samples were collected from the basin and analysed, observing the thickness of the clayey overlay, soil humidity, vegetation, and coarse gravels in the overlay. The respective sampling locations are shown in Fig. 6. The provided information is used in this study to assess the risk of clogging in the MAR basin.

The grain size distribution of the four soil/sediment samples is reported in Fig. 7. The samples were collected from
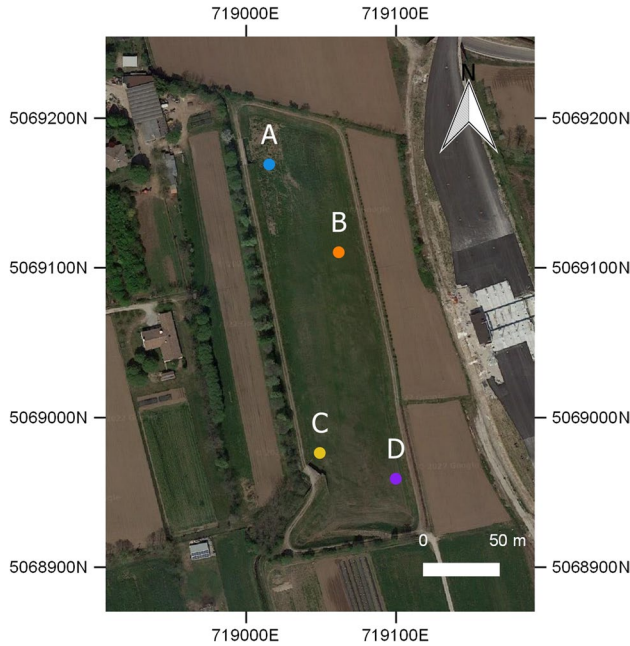

Fig. 6 Sampling spots in the Loria infiltration basin (Italy). The external grid shows the easting and northing UTM-coordinates (WGS 84) in meters

the basin's top layer, up to a depth of 30 cm. The particle size distribution of the finer material is plotted as a separate curve, and the median diameter of 12.33 μm is indicated with a *vertical line*. The finer fraction is differentiated from the sediment matrix, considering the suspended load comprising mainly clay and silt particles. It is here assumed that the analysed fines from the soil samples have likely close origins to the material transported by the river, given the similar granulometric curves in all the finer fractions of the soil samples. The same finer-particle size distribution is thus assumed for the incoming fines from the flood events.

The grain distributions (see Fig. 7) for the sampled sediments allow for quantification of the geometric ratios (d_{50}/D_{50}). For the depositing fines of flood origin, the gradation of the fines is determined by the input of sediments reaching the basin and the expected vertical distribution $f(z)$ from Eqs. (8) and (13). Time series of inflows to the basin are not available for the site, as the pond is filled at irregular intervals during flood events through an adjustable inlet. Assuming the basin reaches its total capacity of 40,000 m³ for each flood event, and given the concentration of suspended solids C (mg/L), $M_{tot} = V_{basin} C$ is the total mass of fines (g) in input to the basin for each flood event. Therefore, from a new input of fines, the expected retained mass with depth per unit volume of porous media (g/cm³) is expressed for each sediment type as in Eq. (15):

Fig. 7 Comparison of fines size distribution and total grain size distributions from the sampled spots A, B, C, D. Median values of the fines size (d_{50}) and the total grain size (D_{50}) are marked with the vertical lines
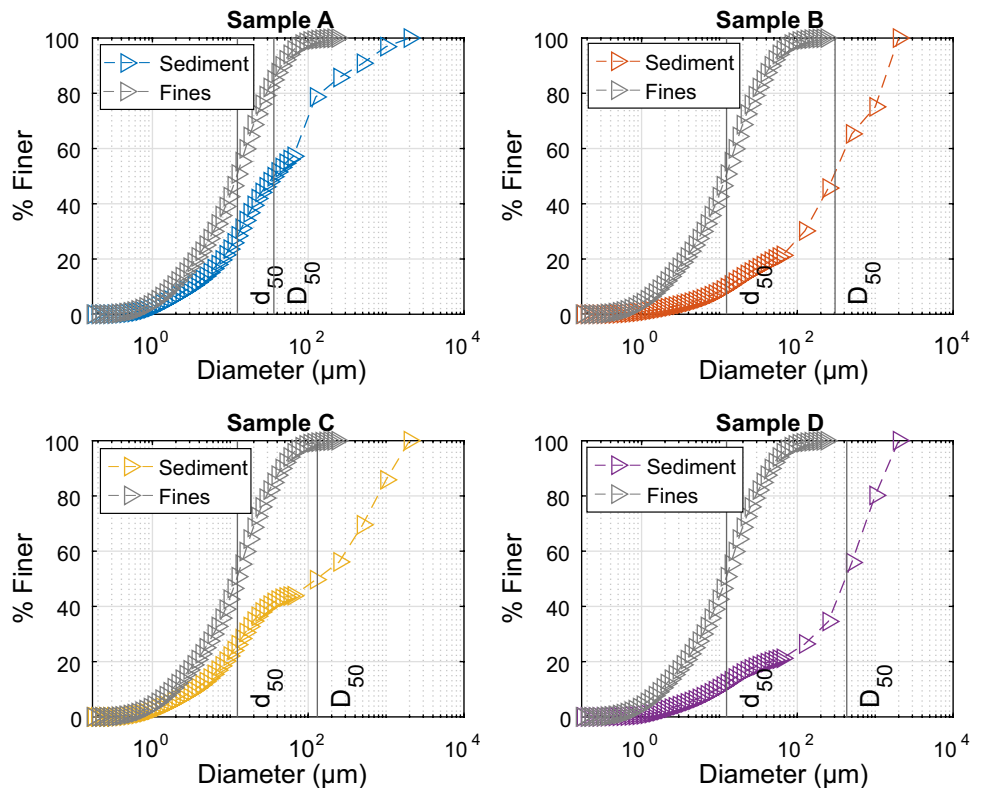
$$\sigma(z,t) = \frac{M_{\text{tot}}(t)}{A_{\text{basin}} l \rho_s} f(z) \quad (19)$$

with A_{basin} the area of the infiltrating basin (cm^2) and l the 1-cm unit depth. Tippelt (2015) reported a peak concentration of 102 mg/L of suspended solids in the river water. For the vulnerability analysis, it is assumed that the peak concentration of fines reaches the basin at each flood event and there is a homogenous infiltration along the basin. For every input of fines following the flooding event, the porous media's initial conditions are updated, namely the porosity, the surface area and tortuosity, according to Eq. (14). The initial porosity, in the absence of field measurements, is here estimated from the coefficient of uniformity (U) through an empirical relationship (Vukovic and Soro 1992):

$$n = 0.255 \left(1 + 0.83^U\right) \quad (20)$$

The initial soil permeability for the native sediments at the sampling locations is derived from the grain size distribution with the Hazen (1893) formula, and a value of permeability of 10^{-8} (cm/s) is considered for the k_{cake} of the clayey material, according to Fitts (2002).

The reductions in soil permeability for the fines material input are expressed in terms of the ratio k/k_0. Figure 8 shows the permeability reductions with soil depth over an accumulation of fines for 50 flooding events.

Applying the Darcy law and a unitary gradient for the downward flow controlled by gravity, the infiltration rate is directly coupled to the decline in soil permeability. The expected reductions in infiltration rate considering the 50 flood events are shown for the four sampling locations in Fig. 9.

Sample A, collected in the proximity of the basin inlet, presents conditions for superficial clogging due to the high presence of fines already in the soil matrix. It is estimated that 95% of new incoming particles are retained superficially from the vertical distribution function. The soil would reach an 83% reduction of the initial infiltration rates after 50 flood events. Similarly, location C, close to the outlet, would exhibit a reduction of 86%. In the north area close to the inlet and along the shortest path to the outlet, soil treatment techniques should be applied to the first upper 5 cm, with frequent scraping schedules to remove the external cake. In location B, in the central part of the basin, the clogging superficial layer would start forming after 37 flooding

Fig. 8 Vertical profiles for the retained fines and reduction in soil permeability after 50 flood events. The vertical line is the clogging depth in cm (Eq. 7). Please note the different scales on the y-axes
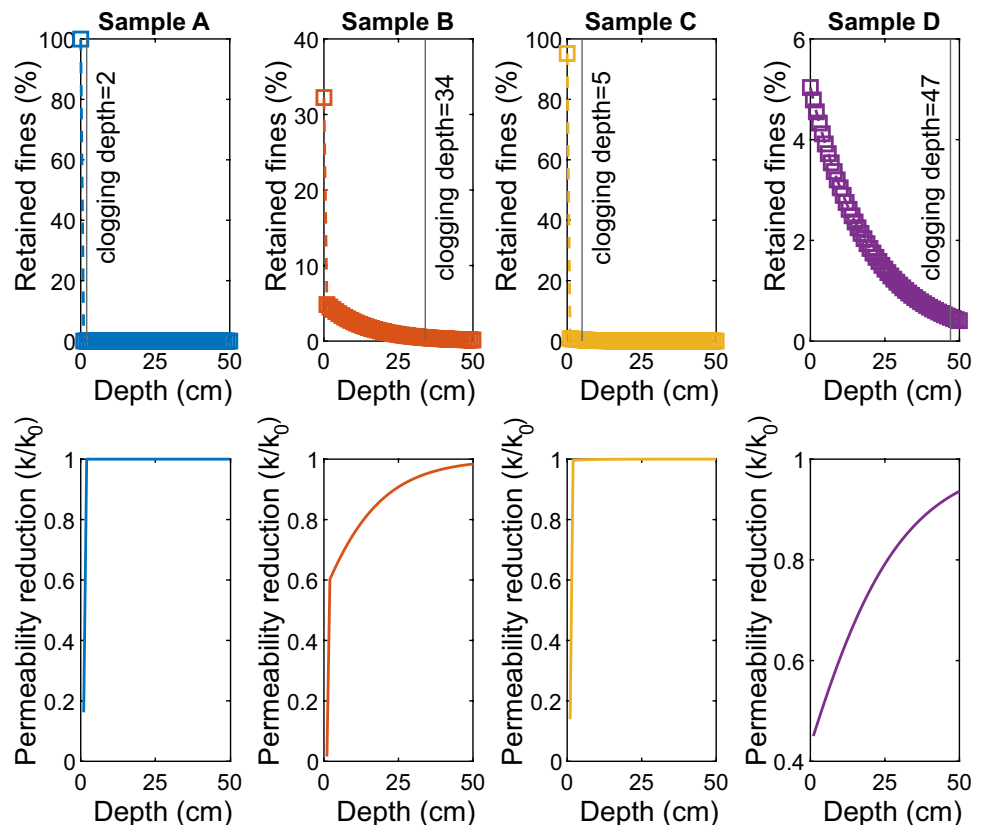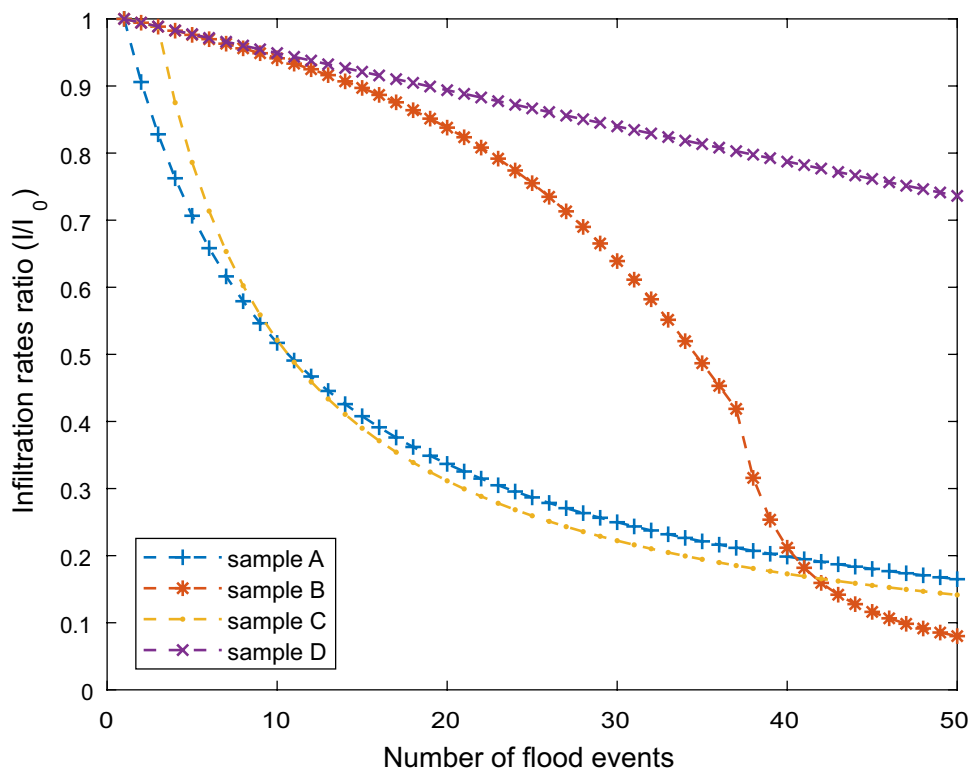
Fig. 9 Predictions in performance of the total infiltration rates, for several potential flood events, at the four sampling locations

events, drastically reducing the infiltration rates. On the other side, sample D, located in the southeast part of the basin, exhibits internal clogging conditions. With 5% of the fines retained superficially, after 50 flooding events, the soil would reach a 26% reduction in infiltration rates; however, further MAR operations could require treating a portion of soil up to a depth of 47 cm. Through the use of site characterisation, soil treatment techniques can be scheduled and programmed in basin zones based on the different lithological characteristics.

Discussion

Predictions of the decline of infiltration rates for MAR sites due to physical clogging are improved by the computation of changes in the soil granulometry and porosity at discretised depths. The main challenge was the quantitative assessment of fines over depth during water recharge. Establishing a generally valid model for the vertical distribution of intrusive fines based on the primary sediment matrix and particles' characteristics leads to a solution suitable for applied hydrogeology purposes. Comparison of experimental results conducted on different column experiments, applicable to MAR conditions, was possible assuming the relative mass of particles to follow an exponential decay with depth. The resulting parameterisation showed that under internal clogging conditions, the percentage of particles retained at the

surface increases linearly with increasing ratio of infiltrated particles of median diameter to grains of median diameter. The exponential decay rate correlates to the amount of fines captured superficially, indicating data from the multiple column experiments to be consistent. Despite the existence of several column experiments for deep bed filtration, the empirical models developed for filter design do not reflect the infiltration basins' operating conditions. Most of these studies provide the residual concentrations in the effluent for colloid transport (diameter size <1 μm) in constant flow rate conditions. Filtration studies often lack information on the retention profile within the porous media. This is indeed a limitation in understanding the straining and deposition processes occurring within the porous media. In recharge basin construction, sandy soils are preferred due to typical infiltration rates being in the range of 0.3–3 m/day (Bouwer 1999; Dillon and Arshad 2016). The interval of interest for this analysis was within a geometric ratio d_{50}/D_{50} of 0.001–0.25. These two reference values correspond to the extreme cases of clay (lower size range 0.98 μm) infiltrating into coarse sand (upper size range 1,000 μm), and to the case of silt (upper size range 62.5 μm) infiltrating into medium sand (lower size range 250 μm), according to the Wentworth scale. In comparison to the profiles under internal clogging conditions from the literature, the additional performed experiments verified that the external cake formation leads to a discrepancy in the relative amount of particles accumulating at the surface. The vertical distribution of fines was

corrected in superficial clogging conditions introducing a retention mass limit at the surface, after which particles accumulate at the top. This solution follows considerations on pore structure concerning median grain diameters and is an approximation for sandy porous media; therefore, there might be limitations for soils with different sediment mixing and compaction. In this regard, the column experiments were performed with porosity values similar to the ones from the literature studies for the same grain size ranges. Although the porous media's compaction likely affects the vertical distribution of fines, the data from the literature provided a negative correlation coefficient ($\rho = -0.0314$) between the porosity and the relative mass at the water–sediment interface. In contrast, this work confirms that straining mechanisms are strongly controlled by the ratio of the diameter size of the suspended particles to the grain diameter size of the porous media. The illustrated findings agree with the qualitative categorisation of Khilar and Fogler (1998) for plugging behaviour due to blocking, bridging and piping, based on previous clogging analysis (Gruesbeck and Collins 1982; Herzig et al. 1970; Muecke 1979). The categorisation is based on ratios determined by the size of fines d_p to the size of the pore constriction d_0. Considering $d_p = d_{50}$ and the average pore diameter (μm) as $d_0 = 0.235\, D_{50}$ valid for sands (Mahmoodlu et al. 2016), the results are consistent with the formation of the external cake for $\frac{d_p}{d_0} > 1$, the occurrence of multiparticle blocking between 0.1–0.01, and piping below 0.01 (Kanti Sen and Khilar 2006). Other authors employ the ratio of the size of the suspended particles to the media size as critical factors in particle straining and reduction in permeability. The results are in good agreement with the threshold of $d_{50}/D_{50} = 0.005$ for initial straining of particles (Bradford et al. 2003; Zaidi et al. 2020) and with $d_{50}/D_{50} = 0.05$ for significant straining (Bradford et al. 2002; Sakthivadivel 1969). It is important to point out that all the selected studies for the analysis measured the d_{50} via laser diffraction. For comparison, the fines' median particle diameter should not be measured with sedimentation methods (Buurman et al. 2001; Di Stefano et al. 2010; Fisher et al. 2017); further discussion is needed to relate the effect of the hydrodynamic conditions in shaping the fines fraction profiles. At lower flow rates, particles would tend to form bridges at pore constrictions, while higher drag forces would break apart these bridges, and particles would be transported deeper into the porous media (Khilar and Fogler 1998). Since this study does not address filtration under high water flow injection, the analysis focuses on comparing the porous media's ability in particle capture, given only the information on the particles' and porous media's median size characteristics. Nevertheless, in constant head conditions, it should be verified whether the median grain diameter D_{50} controls the effect of the hydraulic conductivity and flow rates on the clogging

profiles, confirming the geometric ratio to be the primary predictor. Another point of discussion is whether the particles' concentration in the suspension affects the plugging phenomena, thus altering the retention profile itself. The column experiments of Alem et al. (2014) under constant head conditions were performed for four different concentrations of fines within a range of 0.25–1.5 g/L. By using the same data analysis methods as in section Data analysis', the datasets returned a standard deviation for the $f_{z=0}$ parameter of 0.13%. Considering the concentrations of the experiments summarised in Table 1, the validity of the model reported here is limited to the investigated range of 0.1–1 g/L, which already represents a TSS range of concern in MAR site design. Thus, the results of this work in assessing the vertical distribution of intrusive fines appear to be valid for a broad range of MAR applications. Finally, the field application should not be regarded as a field validation. The sole intention is to clearly show the relevance of the work in evaluating the vulnerability to physical clogging from data commonly collected during site characterizations. In the field application described in section 'MAR application', data are from a site characterization performed in 2015. Additional field measurements of initial soil porosity and hydraulic conductivity should be integrated when possible. Especially, the value of the k_{cake} parameter has a certain relevance in reducing the total permeability of the native sediment, in relation to the original k_0. The model is meant to be applied to determine, in a quick and cost-effective manner, areas of concern to deduce maintenance schemes.

Conclusion

In summary, this work contributes to the research on predicting physical clogging behaviour through an overall model transferable to multiple MAR sites. The novelty of this approach is to not rely on a specific set of parameters determined over a single column experiment, but rather on data easily collectable at the MAR field site. During site characterisation, representative soil samples should be collected, annotating the presence of vertical lithologic discontinuities. The fines are expected to accumulate differently in correspondence with these heterogeneities with distinct retention profiles. A linear relationship defines the expected maximum fraction of fines at the infiltration medium surface and the decrease in particle deposition with depth as a function of the ratio of the infiltrating particle size to the median grain size. When the mass of intruding fines exceeds the retention limit at the surface, this accounts for external cake formation. This mathematical formula can be integrated into clogging models jointly with data on influent suspended solids concentration, frequency of recharge cycles and hydraulic loads, overcoming the gap in estimating

the reductions in infiltration rate. The results for the single soil samples could be extended to the basin area and integrated within an infiltration model, not excluding the fact that more fines would be transported in areas with higher permeability during the infiltration process. Unlike previous studies, the depth-based prediction facilitates the estimation of the maximum operation duration and maintenance costs to remove the soil-clogged layer. Providing information on the expected thickness of the clogged layer makes it possible to address operations of soil replacement and the necessary equipment to restore the infiltration rates for the basin over time. During preliminary analysis, MAR practitioners can use this study's findings to address the risks of physical clogging in multiple infiltration sites.

Declarations

References

Ahfir ND, Hammadi A, Alem A, Wang H, Le Bras G, Ouahbi T (2017) Porous media grain size distribution and hydrodynamic forces effects on transport and deposition of suspended particles. J Environ Sci (China) 53:161–172. https://doi.org/10.1016/j.jes.2016.01.032

Alem A, Ahfir N-D, Elkawafi A, Wang H (2014) Hydraulic operating conditions and particle concentration effects on physical clogging of a porous medium. Transp Porous Media 106(2):303–321. https://doi.org/10.1007/s11242-014-0402-8

Alem A, Elkawafi A, Ahfir N-D, Wang H (2013) Filtration of kaolinite particles in a saturated porous medium: hydrodynamic effects. Hydrogeol J 21(3):573–586. https://doi.org/10.1007/s10040-012-0948-x

Barquero F, Fichtner T, Stefan C (2019) Methods of in situ assessment of infiltration rate reduction in groundwater recharge basins. Water 11(4). https://doi.org/10.3390/w11040784

Becker MW, Bauer B, Hutchinson A (2013) Measuring Artificial Recharge with Fiber Optic Distributed Temperature Sensing. Groundwater 51(5):670–678. https://doi.org/10.1111/j.1745-6584.2012.01006.x

Bennion DB, Bennion DW, Thomas FB, and Bietz RF (1998) Injection water quality: a key factor to successful waterflooding. 37(6). https://doi.org/10.2118/98-06-06

Blazejewski R, Murat-Blazejewska S (1997) Soil clogging phenomena in constructed wetlands with subsurface flow. Water Sci Technol 35(5):183–188. https://doi.org/10.1016/S0273-1223(97)00067-X

Boller MA, Kavanaugh MC (1995) Particle characteristics and head-loss increase in granular media filtration. Water Res 29(4):1139–1149. https://doi.org/10.1016/0043-1354(94)00256-7

Bouwer H (1999) Artificial recharge of groundwater: systems, design, and management, chap 24. In: Hydraulic design handbook. Engineering 360, Albany, NY, 44 pp

Bouwer H (2002) Artificial recharge of groundwater: hydrogeology and engineering. Hydrogeol J 10(1):121–142. https://doi.org/10.1007/s10040-001-0182-4

Bradford SA, Simunek J, Bettahar M, Van Genuchten MT, Yates SR (2003) Modeling colloid attachment, straining, and exclusion in saturated porous media. Environ Sci Technol 37(10):2242. https://doi.org/10.1021/es025899u

Bradford SA, Yates SR, Bettahar M, Simunek J (2002) Physical factors affecting the transport and fate of colloids in saturated porous media. Water Resour Res 38(12):63–1–63–12. https://doi.org/10.1029/2002WR001340

Buurman P, Pape T, Reijneveld JA, De Jong F, Van Gelder E (2001) Laser-diffraction and pipette-method grain sizing of Dutch sediments: correlations for fine fractions of marine, fluvial, and loess samples. Neth J Geosci 80(2):49–57. http://www.njgonline.nl/publish/articles/000035/article.pdf

Carman PC (1937) Fluid flow through granular beds. Trans Inst Chem Eng 15:150–166

Cui Y, Wooster JK, Baker PF, Dusterhoff SR, Sklar LS, Dietrich WE (2008) Theory of fine sediment infiltration into immobile gravel bed. J Hydraul Eng 134(10):1421–1429. https://doi.org/10.1061/(ASCE)0733-9429(2008)134:10(1421)

De Carlo L, Caputo MC, Masciale R, Vurro M, Portoghese I (2020) Monitoring the drainage efficiency of infiltration trenches in fractured and karstified limestone via time-lapse hydrogeophysical approach. Water 12(7):2009. https://doi.org/10.3390/w12072009

Di Stefano C, Ferro V, Mirabile S (2010) Comparison between grain-size analyses using laser diffraction and sedimentation methods. Biosyst Eng 106(2):205–215. https://doi.org/10.1016/j.biosystemseng.2010.03.013

Dillon P (2002) Banking of stormwater, reclaimed water and potable water in aquifers. In: Proc. of the International Groundwater Conference on Sustainable Development and Management of Groundwater Resources in Semi-Arid Region with Special Reference to Hard Rocks: IGC-2002, Dindigul, Tamil Nadu, India, 20–22 February 2002 (pp. 71–80). AA Balkema Publishers.

Dillon P, Arshad M (2016) Managed aquifer recharge in integrated water resource management. In: Jakeman AJ, Barreteau O, Hunt RJ, Rinaudo J-D, Ross A (eds) Integrated groundwater management: concepts, approaches and challenges. Springer, Cham, Switzerland, pp 435–452

Dillon P, Stuyfzand P, Grischek T, Lluria M, Pyne RDG, Jain RC, Bear J, Schwarz J, Wang W, Fernandez E, Stefan C, Pettenati M, van der Gun J, Sprenger C, Massmann G, Scanlon BR, Xanke J, Jokela P, Zheng Y et al (2018) Sixty years of global progress in

managed aquifer recharge. Hydrogeol J 27(1):1–30. https://doi.org/10.1007/s10040-018-1841-z

Dillon P, Vanderzalm J, Page D, Barry K, Gonzalez D, Muthukaruppan M, Hudson M (2016) Analysis of ASR clogging investigations at three Australian ASR sites in a Bayesian context. Water 8(10):442 https://www.mdpi.com/2073-4441/8/10/442

Du X, Ye X, Zhang X (2018) Clogging of saturated porous media by silt-sized suspended solids under varying physical conditions during managed aquifer recharge. Hydrol Process 32(14):2254–2262. https://doi.org/10.1002/hyp.13162

Federico F (2017) Particle migration phenomena related to hydromechanical effects at contact between different materials in embankment dams. In: Sakellariou M (ed.) Granular Materials. IntechOpen. https://doi.org/10.5772/67785

Fisher P, Aumann C, Chia K, O'Halloran N, Chandra S (2017) Adequacy of laser diffraction for soil particle size analysis. PLoS One 12(5):e0176510. https://doi.org/10.1371/journal.pone.0176510

Fitts CR (2002) Groundwater science. Elsevier Science Ltd., Academic Press, 450 pp.

Fontana A, Mozzi P, Marchetti M (2014) Alluvial fans and megafans along the southern side of the Alps. Sediment Geol 301:150–171. https://doi.org/10.1016/j.sedgeo.2013.09.003

Gibson S, Abraham D, Heath R, Schoellhamer D (2009) Vertical gradational variability of fines deposited in a gravel framework. Sedimentology 56(3):661–676. https://doi.org/10.1111/j.1365-3091.2008.00991.x

Glass J, Šimůnek J, Stefan C (2020) Scaling factors in HYDRUS to simulate a reduction in hydraulic conductivity during infiltration from recharge wells and infiltration basins. Vadose Zone J 19(1):e20027. https://doi.org/10.1002/vzj2.20027

Goss D, Smith S, Stewart B, Jones O (1973) Fate of suspended sediment during basin recharge. Water Resour Res 9(3):668–675. https://doi.org/10.1029/WR009i003p00668

Gruesbeck C, Collins R (1982) Entrainment and deposition of fine particles in porous media. SPE J 22(06):847–856. https://doi.org/10.2118/8430-PA

Hazen A (1893) Some physical properties of sands and gravels, with special reference to their use in filtration. In: 24th Annual Rep., Massachusetts State Board of Health, Pub. Doc. No. 34: 539–556. Boston, MA

Herzig JP, Leclerc DM, Goff PL (1970) Flow of suspensions through porous media: application to deep filtration. Ind Eng Chem 62(5):8–35. https://doi.org/10.1021/ie50725a003

Huston DL, Fox JF (2015) Clogging of fine sediment within gravel substrates: dimensional analysis and macroanalysis of experiments in hydraulic flumes. J Hydraul Eng 141(8). https://doi.org/10.1061/(asce)hy.1943-7900.0001015

Hutchison A, Milczarek M, Banerjee M (2013) Clogging phenomena related to surface water recharge facilities. In: Martin R (ed.) Clogging issues associated with managed aquifer recharge methods. IAH Commission on Managing Aquifer Recharge. 95–106. https://recharge.iah.org/files/2015/03/Clogging_Monograph.pdf

Kanti Sen T, Khilar KC (2006) Review on subsurface colloids and colloid-associated contaminant transport in saturated porous media. Adv Colloid Interf Sci 119(2–3):71–96. https://doi.org/10.1016/j.cis.2005.09.001

Khilar KC, Fogler HS (1998) Migration of fines in porous media. Kluwer Academic Publishers, Dordrecht, The Netherlands

Kozeny J (1927) Uber kapillare Leitung der Wasser in Boden [About capillary conduction of water in soil]. Royal Academy of Science, Vienna Proc Class I 136:271–306

Locke M, Indraratna B, Adikari G (2001) Time-dependent particle transport through granular filters. J Geotech Geoenviron 127(6):521–529. https://doi.org/10.1061/(ASCE)1090-0241(2001)127:6(521)

Mahmoodlu MG, Raoof A, Sweijen T, Van Genuchten M (2016) Effects of sand compaction and mixing on pore structure and the unsaturated soil hydraulic properties. Vadose Zone J 15. https://doi.org/10.2136/vzj2015.10.0136

Martin R (ed.) (2013) Clogging issues associated with managed aquifer recharge methods. IAH Commission on Managing Aquifer Recharge. https://recharge.iah.org/files/2015/03/Clogging_Monograph.pdf

Mawer C, Parsekian A, Pidlisecky A, Knight R (2016) Characterizing heterogeneity in infiltration rates during managed aquifer recharge. Ground Water 54(6):818–829. https://doi.org/10.1111/gwat.12423

McDowell-Boyer LM, Hunt JR, Sitar N (1986) Particle transport through porous media. Water Resour Res 22(13):1901–1921. https://doi.org/10.1029/WR022i013p01901

Muecke TW (1979) Formation fines and factors controlling their movement in porous media. J Petrol Technol 31(02):144–150. https://doi.org/10.2118/7007-PA

Nenna V, Pidlisecky A, Knight R (2014) Monitoring managed aquifer recharge with electrical resistivity probes. Interpretation 2(4):T155–T166. https://doi.org/10.1190/INT-2013-0192.1

Okubo T, Matsumoto J (1983) Biological clogging of sand and changes of organic constituents during artificial recharge. Water Res 17(7):813–821. https://doi.org/10.1016/0043-1354(83)90077-5

P.A.T.I. (2013) Relazione geologica ed idrogeologica PATI Loria e Castello di Godego [Geological and hydrogeological relationship of PATI Loria and Castello di Godego]. http://www.prc.loria.geonweb.com/documents/elaborati_QC/Relazione%20geologica%20ed%20idrogeologica.pdf. Accessed December 2022

Pyne RDG (1995) Groundwater Recharge and Wells: A Guide to Aquifer Storage Recovery (1st ed.). CRC Press. https://doi.org/10.1201/9780203719718

Racz AJ, Fisher AT, Schmidt CM, Lockwood BS, Los HM (2012) Spatial and temporal infiltration dynamics during managed aquifer recharge. Ground Water 50(4):562–570. https://doi.org/10.1111/j.1745-6584.2011.00875.x

Reddi LN, Ming X, Hajra MG, Lee IM (2000) Permeability reduction of soil filters due to physical clogging. J Geotech Geoenviron 126(3):236–246. https://doi.org/10.1061/(ASCE)1090-0241(2000)126:3(236)

Ross A, Hasnain S (2018) Factors affecting the cost of managed aquifer recharge (MAR) schemes. Sustain Water Resources Manag 4(2):179–190. https://doi.org/10.1007/s40899-017-0210-8

Sakthivadivel R (1969) Clogging of a granular porous medium by sediment. Rep. HEL 15–7, 106 pp., Hydraul. Eng. Lab., Univ. of Calif.,Berkeley, CA

Sprenger C, Hartog N, Hernández M, Vilanova E, Grützmacher G, Scheibler F, Hannappel S (2017) Inventory of managed aquifer recharge sites in Europe: historical development, current situation and perspectives. Hydrogeol J 25(6):1909–1922. https://doi.org/10.1007/s10040-017-1554-8

Tang Y, Yao X, Chen Y, Zhou Y, Zhu DZ, Zhang Y, Zhang T, Peng Y (2020) Experiment research on physical clogging mechanism in the porous media and its impact on permeability. Granul Matter 22(2). https://doi.org/10.1007/s10035-020-1001-8

Tippelt T (2015) Investigation of the influence of fine sediment input during flooding events on the long-term infiltration capacity of the Loria infiltration basin (Italy). MSc Thesis, Institute of Geophysics and Geology, Leipzig University, Leipzig, Germany

Torkzaban S, Bradford SA, Vanderzalm JL, Patterson BM, Harris B, Prommer H (2015) Colloid release and clogging in porous media: effects of solution ionic strength and flow velocity. J Contam Hydrol 181:161–171. https://doi.org/10.1016/j.jconhyd.2015.06.005

Ulusoy İ, Dahlin T, Bergman B (2015) Time-lapse electrical resistivity tomography of a water infiltration test on Johannishus Esker, Sweden. Hydrogeol J 23(3):551–566. https://doi.org/10.1007/s10040-014-1221-2

Vukovic M, Soro A (1992) Determination of hydraulic conductivity of porous media from grain-size composition. Water Resources Publications, Littleton, CO

Wang Z, Du X, Yang Y, Ye X (2012) Surface clogging process modeling of suspended solids during urban stormwater aquifer recharge. J Environ Sci 24(8):1418–1424. https://doi.org/10.1016/s1001-0742(11)60961-3

Xie Y, Wang Y, Huo M, Geng Z, Fan W (2020) Risk of physical clogging induced by low-density suspended particles during managed aquifer recharge with reclaimed water: evidences from laboratory experiments and numerical modeling. Environ Res 186:109527. https://doi.org/10.1016/j.envres.2020.109527

Zaidi M, Ahfir N-D, Alem A, El Mansouri B, Wang H, Taibi S, Duchemin B, Merzouk A (2020) Assessment of clogging of managed aquifer recharge in a semi-arid region. Sci Total Environ 730:139107. https://doi.org/10.1016/j.scitotenv.2020.139107

Zhang H, Xu Y, Kanyerere T (2020) A review of the managed aquifer recharge: historical development, current situation and perspectives. Phys Chem Earth, parts A/B/C, 118–119:102887. https://doi.org/10.1016/j.pce.2020.102887